

Graphene Thickness Determination Using Reflection and Contrast Spectroscopy

Z. H. Ni,[†] H. M. Wang,[§] J. Kasim,[‡] H. M. Fan,^{†,‡} T. Yu,[‡] Y. H. Wu,[§]
Y. P. Feng,[†] and Z. X. Shen^{*,‡}

Department of Physics, National University of Singapore, 2 Science Drive 3, Singapore 117542, Division of Physics and Applied Physics, School of Physical and Mathematical Sciences, Nanyang Technological University, 1 Nanyang Walk, Block 5, Level 3, Singapore 637616, and Department of Electrical and Computer Engineering, National University of Singapore, 4 Engineering Drive 3, Singapore 117576

Received May 28, 2007; Revised Manuscript Received July 16, 2007

ABSTRACT

We have clearly discriminated the single-, bilayer-, and multiple-layer graphene (<10 layers) on Si substrate with a 285 nm SiO₂ capping layer by using contrast spectra, which were generated from the reflection light of a white light source. Calculations based on Fresnel's law are in excellent agreement with the experimental results (deviation 2%). The contrast image shows the reliability and efficiency of this new technique. The contrast spectrum is a fast, nondestructive, easy to be carried out, and unambiguous way to identify the numbers of layers of graphene sheet. We provide two easy-to-use methods to determine the number of graphene layers based on contrast spectra: a graphic method and an analytical method. We also show that the refractive index of graphene is different from that of graphite. The results are compared with those obtained using Raman spectroscopy.

The recent success in extracting graphite sheets in multiple layers, and even monolayer graphene, from highly ordered pyrolytic graphite (HOPG) using a technique called micro-mechanical cleavage^{1,2} has stimulated great interest in both the fundamental physics study and the potential applications of graphene.³ Graphene has a two-dimensional (2D) crystal structure, which is the basic building block for other sp² carbon nanomaterials, such as nanographite sheets and carbon nanotubes. The peculiar properties of graphene arise from its unique electronic band structure, in which the conduction band touches the valence band at two points (*K* and *K'*)^{4,5} in the Brillouin zone, and in the vicinity of these points, the electron energy has a linear relationship with the wavevector, $E = \hbar kv_f$. Therefore, electrons in an ideal graphene sheet behave like massless Dirac–Fermions.^{6,7} Some of these unique properties have been observed experimentally^{8–21} and many new ideas^{22–29} about the fundamental physics and device applications of single- and multiple-layer graphene have been proposed. Presently micromechanical cleavage is

still the most effective way to produce high-quality graphene sheets, and a quick and precise method for determining the thickness of graphene sheets is essential for speeding up the research and exploration of graphene. Although atomic force microscopy (AFM) measurement is the most direct way to identify the number of layers of graphene, the method has a very slow throughput and may also cause damage to the crystal lattice during measurement. Furthermore, an instrumental offset of ~0.5 nm (caused by different interaction forces) always exists, which is even larger than the thickness of a monolayer graphene and data fitting is required to extract the true thickness of graphene sheets.³⁰ Unconventional quantum Hall effects^{8–10} are often used to differentiate monolayer and bilayer graphene from multiple layers. However, it is not a practical and efficient way. Researchers have attempted to develop more efficient ways to identify different layers of graphene without destroying the crystal lattice. Raman spectroscopy is a potential candidate for nondestructive and quick inspection of the thickness of graphene.^{30–32} Unfortunately, the differences between two layers and a few layers of graphene sheets are not obvious and unambiguous in Raman spectra. Another possible way is to identify graphene layers of different thickness with the “naked eye” with an optical microscope. However, this is

* Corresponding author. E-mail: zexiang@ntu.edu.sg.

[†] Department of Physics, National University of Singapore.

[‡] Division of Physics and Applied Physics, School of Physical and Mathematical Sciences, Nanyang Technological University.

[§] Department of Electrical and Computer Engineering, National University of Singapore.

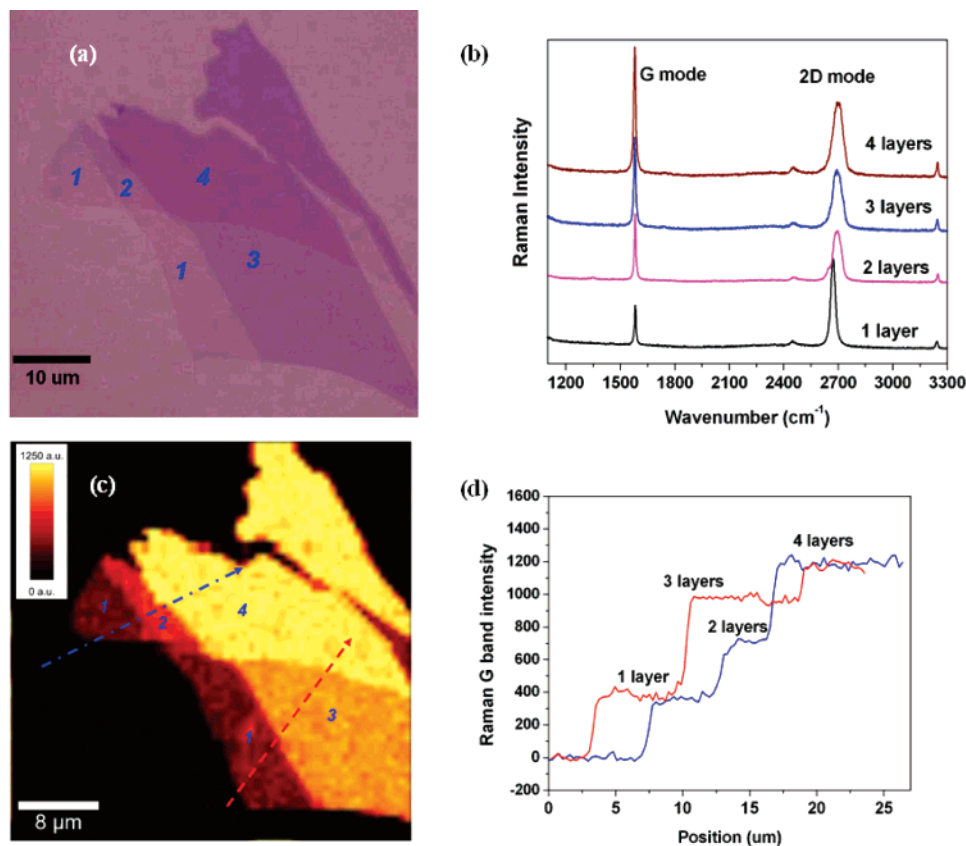


Figure 1. (a) Optical image of graphene with one, two, three, and four layers. (b) Raman spectra as a function of number of layers. (c) Raman image plotted by the intensity of G band. (d) The cross section of Raman image, which corresponds to the dash lines.

not a quantitative method because the color/contrast often varies from one laboratory to another.^{1,9}

In this contribution, we report a direct method for efficient and accurate inspection of the graphene sheet using contrast spectrum. The contrast between the graphene layers and the SiO₂/Si substrate, which makes the graphene visible, was generated from a reflection spectrum by using a normal white light source. Clear contrast difference for graphene sheets from one to ten layers can be observed. Calculations based on Fresnel's equations have been carried out, and the results show excellent agreement with the experimental data. The contrast image provides good evidence that this new method is an efficient and unambiguous way to identify the number of graphene layers.

The graphene samples were prepared by micromechanical cleavage and transferred to a Si wafer with a 285 nm SiO₂ capping layer.¹ An optical microscope was used to locate the graphene sheet, and the thickness was further confirmed by Raman spectra/image. In the reflection experiments, incident light was emitted from a normal white light source (tungsten halogen lamp, excitation range from 350 to 850 nm, through a 1 mm aperture). The reflected light was collected using backscattering configuration (with a 100 μm pinhole) and directed to a 150 lines/mm grating and detected with a TE-cooled charge-coupled-device (CCD). The obtained reflection spectra were compared with that of a background spectrum from SiO₂/Si to generate the contrast spectra. The Raman spectra were carried out with a WITec CRM200 Raman system. The excitation source is 532 nm

laser (2.33 eV) with a laser power below 0.1 mW on the sample to avoid laser induced heating. A 100× objective lens with a NA = 0.95 was used both in the Raman and in reflection experiments, and the spot sizes of 532 nm laser and white light were estimated to be 500 nm and 1 μm, respectively, which we determined by using a scanning edge method.³³ For the contrast and Raman image, the sample was placed on an *x*-*y* piezostage and scanned under the illumination of laser and white light. The Raman and reflection spectra from every spot of the sample were recorded. The stage movement and data acquisition were controlled using ScanCtrl Spectroscopy Plus software from WITec GmbH, Germany. Data analysis was done using WITec Project software.

Figure 1a shows the optical image of a graphene sample on the SiO₂/Si substrate. The graphene sheet shows four different contrast regions, which can be understood as having four different thicknesses. The Raman spectra were then taken from different regions of the sample, and the results are shown in Figure 1b. As has been proposed by Ferrari et al., the second-order Raman 2D band is sensitive to the number of layers of graphene^{31,32} and the 2D band of single layer graphene is very sharp and symmetric. For bilayer and multiple-layer graphenes, the 2D band becomes much broader mainly due to the change of electronic structure of graphene, which affects the process of double resonance effect.³⁴ In our Raman spectra, the sharp 2D band of the single layer graphene can be clearly observed and distinguished from bilayer and multiple layer. However, the

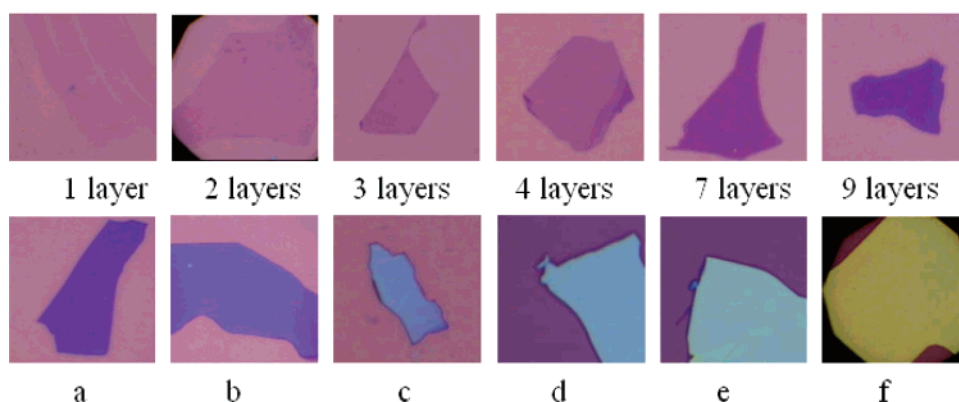
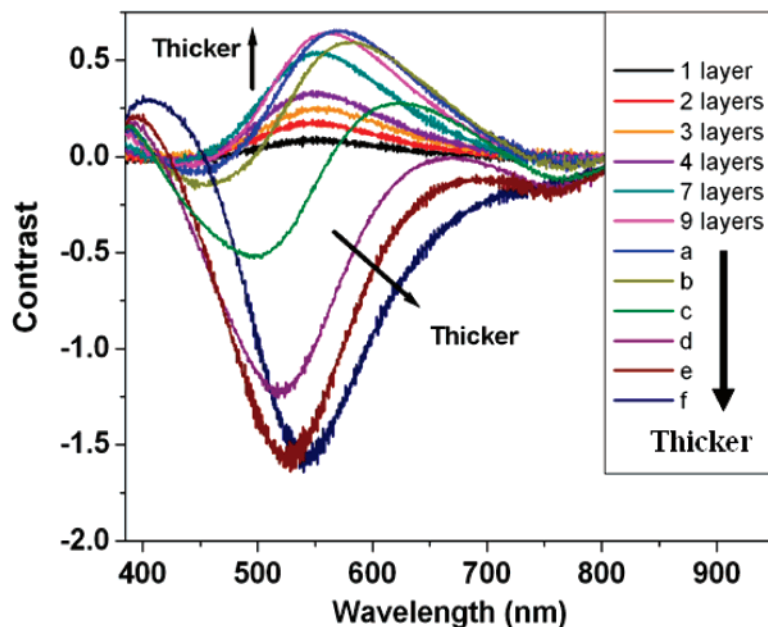


Figure 2. The contrast spectra of graphene sheets with different thicknesses, together with the optical image of all the samples. Besides the samples with one, two, three, four, seven, and nine layers, samples a, b, c, d, e, and f are more than 10 layers and the thickness increases from a to f. The arrows in the graph show the trend of curves in terms of the thicknesses of graphene sheets.

difference in the 2D band is not obvious for two to four layers. A clear difference between those layers is that G band intensity shows an increase with the number of layers (the spectra are recorded under the same condition). Once the single-layer graphene is identified by the 2D band of Raman scattering, we can further identify different layers of graphene from the G band intensity plot, as shown in Figure 1c. This can be done as the intensity of the G band almost linearly increases with the number of layers of graphene.³² Figure 1d plots the Raman intensity of the G band along two dash lines drawn in Figure 1c. It is obvious that the graphene sheet contains one, two, three, and four layers. These can be compared with the contrast spectrum/image discussed later.

Figure 2 shows the contrast spectra for different thicknesses of graphene sheets, together with the optical images of all the samples used. Besides the samples with one, two, three, four, seven, and nine layers, samples a, b, c, d, e, and f are more than 10 layers thick and the thickness increases from a to f. The contrast spectra are obtained by the calculation $C(\lambda) = (R_0(\lambda) - R(\lambda))/R_0(\lambda)$, where $R_0(\lambda)$ is the reflection spectrum from the SiO₂/Si substrate and $R(\lambda)$ is the reflection spectrum from graphene sheet. With this

method, the contrast across the whole visible range (with a spectrum resolution higher than 1 nm) can be recorded continually and no bandpass filter, which was used in ref 35, is needed. Although one can observe different colors/contrasts for graphene sheets of different thickness using the optical image with the “naked eye”, graphene’s visibility strongly varies from one laboratory to another and it relies on experience of the observer. Contrast spectra can make it quantitative and accurate. The contrast spectrum for single-layer graphene has a peak centered at 550 nm, which is in the green-orange range and it makes the single-layer graphene visible. The contrast peak position is almost unchanged (550 nm) with increasing layers up to 10. The contrast for single-layer graphene is about 0.09 ± 0.005 , and it increases with the number of layers, for example, 0.175 ± 0.005 , 0.255 ± 0.010 , and 0.330 ± 0.015 for two, three, and four layers, respectively. For graphene of around 10 layers in thickness, the contrast of the sample saturates and the contrast peak shifts toward higher wavelength (samples a and b). For samples with a larger number of layers (c–f), negative contrast occurs. This can easily be understood that these samples are so thick that the reflections from their

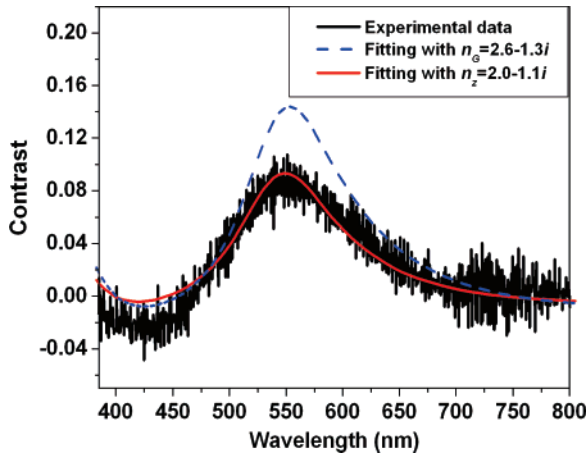


Figure 3. The contrast spectrum of experimental data (black line), the simulation result using $n = 2.0 - 1.1i$ (red line), and the simulation result using $n_G = 2.6 - 1.3i$ (dash line).

surface become more intense than that from the SiO_2/Si substrate, resulting in negative value contrast.

The origin of the contrast can be explained by Fresnel's equations. Consider the incident light from air ($n_0 = 1$) onto a graphene, SiO_2 , and Si trilayer system. The reflected light intensity from the trilayer system can then be described by^{35,36}

$$R(\lambda) = r(\lambda) r^*(\lambda) \quad (1)$$

$$r(\lambda) = \frac{r_a}{r_b} \quad (2)$$

$$r_a = (r_1 e^{i(\beta_1 + \beta_2)} + r_2 e^{-i(\beta_1 - \beta_2)} + r_3 e^{-i(\beta_1 + \beta_2)} + r_1 r_2 r_3 e^{i(\beta_1 - \beta_2)}) \quad (3)$$

$$r_b = (e^{i(\beta_1 + \beta_2)} + r_1 r_2 e^{-i(\beta_1 - \beta_2)} + r_1 r_3 e^{-i(\beta_1 + \beta_2)} + r_2 r_3 e^{i(\beta_1 - \beta_2)}) \quad (4)$$

where $r_1 = (n_0 - n_1)/(n_0 + n_1)$, $r_2 = (n_1 - n_2)/(n_1 + n_2)$, and $r_3 = (n_2 - n_3)/(n_2 + n_3)$ are the reflection coefficients for different interfaces and $\beta_1 = 2\pi n_1(d_1/\lambda)$ and $\beta_2 = 2\pi n_2(d_2/\lambda)$ are the phase differences when light passes through the media which is determined by the path difference of two neighboring interfering light beams. The thickness of the graphene sheet can be estimated as $d_l = N\Delta d$, where N represents the number of layers and Δd is the thickness of single layer graphene ($\Delta d = 0.335 \text{ nm}$).^{37,38} The refractive index of graphene may differ from that of bulk graphite ($n_G = 2.6 - 1.3i$),³⁵ which can be used as a fitting parameter. The thickness of SiO_2 , d_2 , is 285 nm, with a maximum 5% error. The refractive index of SiO_2 , n_2 , is wavelength dependent, which was taken from ref 39. The Si substrate can be considered semi-infinite and the refractive index of Si, n_3 , is also wavelength dependent.³⁹ The reflection from SiO_2 background, $R_0(\lambda)$, was calculated by using $n_1 = n_0 = 1$, and $d_1 = 0$.

The calculated contrast spectra of single layer graphene are shown in Figure 3. The optimized simulation result was obtained with the refractive index of a single-layer graphene $n_z = 2.0 - 1.1i$, whereas the simulation result using the bulk graphite value of $n_G(2.6 - 1.3i)$ shows large deviation from

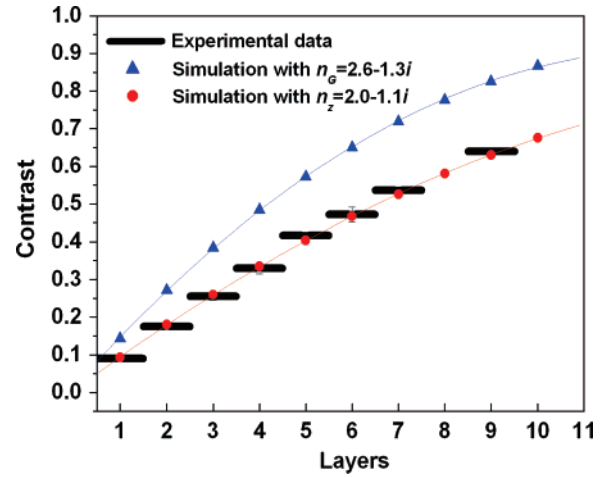


Figure 4. The contrast simulated by using both n_G (blue triangles) and n_z (red circles), the fitting curve for the simulations (blue and red lines), and our experiment data (black thick lines), respectively, for 1–10 layers of graphene.

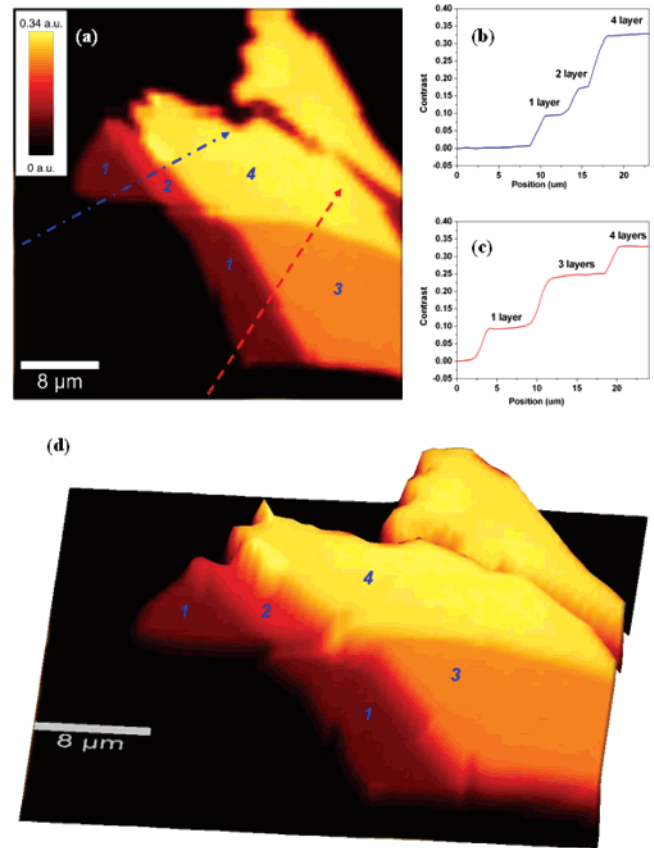


Figure 5. (a) The contrast image of the sample. (b, c) The cross section of contrast image, which corresponds to the dash lines. The contrast values of each thickness agree well with the contrast values of one to four layers as shown in Figure 4. (d) The 3D contrast image, which shows a better perspective view of the sample.

our experimental data. The variation of the refractive index of graphene from that of graphite may be ascribed to the decrease of interlayer interaction when the sample is ultrathin. Using the optimized refractive index n_z , we calculated the contrast spectra of 2–10 layers and a significant improvement of agreement between the fitting results and the

experimental data was readily achieved as shown in Figure 4. The deviation between experimental results and simulation is only 2%. With this technique, the thickness of an unknown graphene sheet can be determined directly by comparing the contrast value with the standard values shown in Figure 4. Alternatively, it can be obtained using the following equation

$$C = 0.0046 + 0.0925N - 0.00255N^2 \quad (5)$$

where N (≤ 10) is the number of layers of graphene sheet.

Our technique does not need a single-layer graphene as reference (as in Raman), and it does not have an instrument offset problem caused by different interaction forces between probe and medium (as in AFM).³⁰ Moreover, the simulation shows that the highest contrast of graphene sheet is almost unchanged for the thickness of SiO₂ substrate between 280 and 320 nm. Thus, our results can be applied directly to a 300 nm SiO₂ capping layer, which is also commonly used. With simple modification, our technique can also be used to identify the number of graphene layers on a 90 nm SiO₂ substrate, which, as suggested by Blake et al.,³⁵ may provide better contrast.

In order to demonstrate the effectiveness of the contrast spectra in graphene thickness determination, we carried out contrast imaging, which was performed by scanning the sample under white light illumination, with an x - y piezostage and recording the reflection spectrum from every spot of the sample. As shown in Figure 5a, distinct contrast for different thicknesses of graphene can be observed from the image. It is worth noting that the contrast image measurement can be done in a few minutes. Parts b and c of Figure 5 show contrast along the two dash lines on the image. The contrast value for each thickness agrees well with those shown in Figure 4. Using eq 5, the N values along the two dash lines are calculated, where the N along the blue line is 0.99, 1.93, and 3.83 and along the red line is 0.98, 2.89 and 3.94. Again our results show excellent agreement. The 3D contrast image is shown in Figure 5d, which gives a better perspective view of the sample.

In summary, we have demonstrated that by using contrast spectra, we can easily determine the number of graphene layers. We have also calculated the contrast using Fresnel's equations, and the results show an excellent match with the experimental data. From the simulation, we extracted the refractive index of graphene below 10 layers as $n_z = 2.0 - 1.1i$, which is different from that of bulk graphite. Our experimental values can be directly used as a standard to identify the thickness of graphene sheet on Si substrate with ~ 300 nm SiO₂ capping layer. We have also given an analytical expression for determining number of layers. From the contrast image, we have demonstrated the effectiveness of this new technique. Although current research mainly focuses on the single and bilayer graphene, we believe that multiple layers (less than 10 layers) of graphene also have interesting properties as they still exhibit the two-dimensional properties.³ Reflection and contrast spectroscopy provides a fast, nondestructive, easy-to-use, and accurate method to

identify the number of graphene layers (below 10 layers), which helps future research and application of graphene.

References

- (1) Novoselov, K. S.; Geim, A. K.; Morozov, S. V.; Jiang, D.; Zhang, Y.; Dubonos, S. V.; Grigorieva, I. V.; Firsov, A. A. *Science* **2004**, *306*, 666.
- (2) Novoselov, K. S.; Jiang, D.; Schedin, F.; Booth, T. J.; Khotkevich, V. V.; Morozov, S. V.; Geim, A. K. *Proc. Natl. Acad. Sci. U.S.A.* **2005**, *102*, 10451.
- (3) Geim, A. K.; Novoselov, K. S. *Nat. Mater.* **2007**, *6*, 183.
- (4) Wallace, P. R. *Phys. Rev.* **1947**, *71*, 622.
- (5) Slonczewski, J. C.; Weiss, P. R. *Phys. Rev.* **1958**, *109*, 272.
- (6) Semenoff, G. W. *Phys. Rev. Lett.* **1984**, *53*, 2449.
- (7) Haldane, F. D. M. *Phys. Rev. Lett.* **1988**, *61*, 2015.
- (8) Novoselov, K. S.; Geim, A. K.; Morozov, S. V.; Jiang, D.; Katsnelson, M. I.; Grigorieva, I. V.; Dubonos, S. V.; Firsov, A. A. *Nature* **2005**, *438*, 197.
- (9) Zhang, Y. B.; Tan, Y. W.; Stormer, H. L.; Kim, P. *Nature* **2005**, *438*, 201.
- (10) Novoselov, K. S.; Jiang, Z.; Zhang, Y.; Morozov, S. V.; Stormer, H. L.; Zeitler, U.; Maan, J. C.; Boebinger, G. S.; Kim, P.; Geim, A. K. *Science* **2007**, *315*, 1379.
- (11) Novoselov, K. S.; McCann, E.; Morozov, S. V.; Fal'ko, V. I.; Katsnelson, M. I.; Zeitler, U.; Jiang, D.; Schedin, F.; Geim, A. K. *Nat. Phys.* **2006**, *2*, 177.
- (12) Bunch, S. J.; van der Zande, A. M.; Verbridge, S. S.; Frank, I. W.; Tanenbaum, D. M.; Parpia, J. M.; Craighead, H. G.; McEuen, P. L. *Science* **2007**, *315*, 490.
- (13) Heersche, H. B.; Jarillo-Herrero, P.; Oostinga, J. B.; Vandersypen, L. M. K.; Morpurgo, A. F. *Nature* **2007**, *446*, 56.
- (14) Meyer, J. C.; Geim, A. K.; Katsnelson, M. I.; Novoselov, K. S.; Booth, T. J.; Roth, S. *Nature* **2007**, *446*, 60.
- (15) Ohta, T.; Bostwick, A.; Seyller, T.; Horn, K.; Rotenberg, E. *Science* **2006**, *313*, 951.
- (16) Bostwick, A.; Ohta, T.; Seyller, T.; Horn, K.; Rotenberg, E. *Nat. Phys.* **2007**, *3*, 36.
- (17) Hill, E. W.; Geim, A. K.; Novoselov, K. S.; Schedin, F.; Blake, P. *IEEE Trans. Magn.* **2006**, *42*, 2694.
- (18) Chen, Z. H.; Lin, Y. M.; Rooks, M. J.; Avouris, P. Preprint at <http://arxiv.org/abs/cond-mat/0701599> (2007).
- (19) Han, M. Y.; Oezylmaz, B.; Zhang, Y. B.; Kim, P. Preprint at <http://arxiv.org/abs/cond-mat/0702511> (2007).
- (20) Berger, C.; Song, Z. M.; Li, X. B.; Wu, X. S.; Brown, N.; Naud, C.; Mayou, D.; Li, T. B.; Hass, J.; Marchenkov, A. N.; Conrad, E. H.; First, P. N.; de Heer, W. A. *Science* **2006**, *312*, 1191.
- (21) Castro, E. V.; Novoselov, K. S.; Morozov, S. V.; Peres, N. M. R.; Lopes dos Santos, J. M. B.; Nilsson, J.; Guinea, F.; Geim, A. K.; Castro Neto, A. H. Preprint at <http://arxiv.org/abs/cond-mat/0611342> (2006).
- (22) Peres, N. M. R.; Guinea, F.; Castro, N. A. H. *Phys. Rev. B* **2006**, *73*, 125411.
- (23) Nilsson, J.; Castro Neto, A. H.; Guinea, F.; Peres, N. M. R. Preprint at <http://arxiv.org/abs/cond-mat/0604106> (2006).
- (24) Titov, M.; Beenakker, C. W. J. *Phys. Rev. B* **2006**, *74*, 041401.
- (25) Son, Y. W.; Cohen, M. L.; Louie, S. G. *Nature* **2006**, *444*, 347.
- (26) Katsnelson, M. I.; Novoselov, K. S.; Geim, A. K. *Nat. Phys.* **2006**, *2*, 620.
- (27) Cheianov, V. V.; Fal'ko, V.; Altshuler, B. L. *Science* **2007**, *315*, 1252.
- (28) Rycerz, A.; Tworzydło, J.; Beenakker, C. W. J. *Nat. Phys.* **2007**, *3*, 172.
- (29) Trauzettel, B.; Bulaev, D. V.; Loss, D.; Burkard, G. *Nat. Phys.* **2007**, *3*, 192.
- (30) Gupta, A.; Chen, G.; Joshi, P.; Tadigadapa, S.; Eklund, P. C. *Nano Lett.* **2006**, *6*, 2667.
- (31) Ferrari, A. C.; Meyer, J. C.; Scardaci, V.; Casiraghi, C.; Lazzeri, M.; Mauri, F.; Piscanec, S.; Jiang, D.; Novoselov, K. S.; Roth, S.; Geim, A. K. *Phys. Rev. Lett.* **2006**, *97*, 187401.
- (32) Graf, D.; Molitor, F.; Ensslin, K.; Stampfer, C.; Jungen, A.; Hierold, C.; Wirtz, L. *Nano Lett.* **2007**, *7*, 238.
- (33) Veshapidze, G.; Trachy, M. L.; Shah, M. H.; DePaola, B. D. *Appl. Opt.* **2006**, *45*, 8197.
- (34) Thomsen, C.; Reich, S. *Phys. Rev. Lett.* **2000**, *85*, 5214.

- (35) Blake, P.; Novoselov, K. S.; Castro Neto, A. H.; Jiang, D.; Yang, R.; Booth, T. J.; Geim, A. K.; Hill, E. W. Preprint at <http://arxiv.org/abs/cond-mat/0705.0259> (2007).
- (36) Anders, H. *Thin Films in Optics*; Focal Press: London, 1967.
- (37) Kelly, B. T. *Physics of Graphite*; Applied Science: London, 1981.
- (38) Dresselhaus, M. S.; Dresselhaus, G.; Eklund, P. C. *Science of Fullerenes and Carbon Nanotubes*; Academic Press: San Diego, CA, 1996; p 965.
- (39) Palik, E. D. *Handbook of Optical Constants of Solids*; Academic Press: New York, 1991.

NL071254M